Supplementary Information

Metal selectivity and translocation mechanism characterization in proteoliposomes of the transmembrane NiCoT transporter NixA from *Helicobacter pylori*

Jayoh A. Hernandez[1], Paul S. Micus[1], Sean Alec Lois Sunga[1], Luca Mazzei[2], Stefano Ciurli[2], Gabriele Meloni[1*]

[1]Department of Chemistry and Biochemistry, The University of Texas at Dallas, Richardson, TX 75080, USA.
[2] Laboratory of Bioinorganic Chemistry, Department of Pharmacy and Biotechnology, University of Bologna, Bologna, Italy

*E-mail: gabriele.meloni@utdallas.edu.

Figure S1. Detergent screening for the solubilization NixA from isolated membranes (SUP – supernatant; PEL – pellet). Six different detergents were utilized to determine the extraction efficiency. For details see Material and Methods.
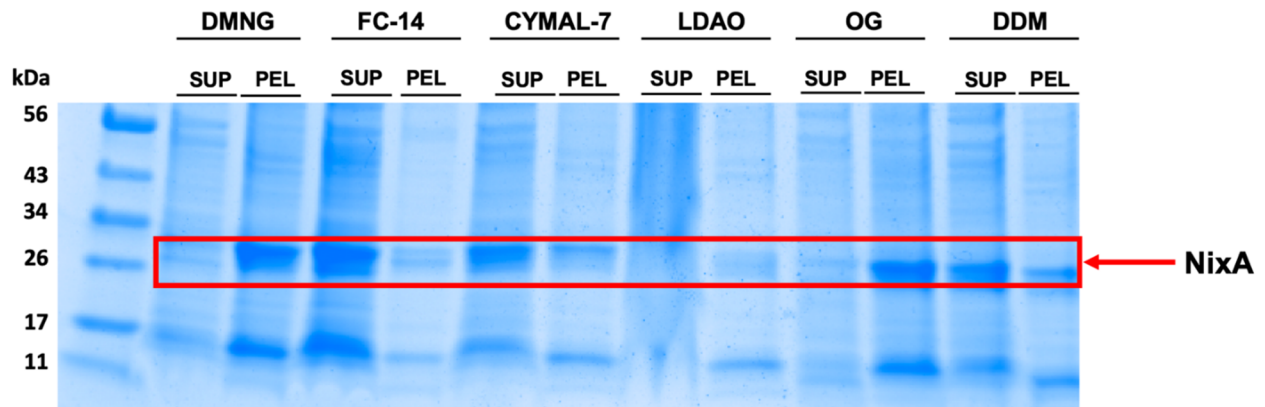
DMNG – Decyl Maltose Neopentyl Glycol
FC-14 – Fos Choline-14
CYMAL-7 – 7-Cyclohexyl-1-Heptyl-β-D-Maltoside
LDAO – Lauryldimethylamine-N-Oxide
OG – n-octyl-β-D-glucopyranoside
DDM – n-dodecyl-β-D-maltopyranoside

Figure S2. NixA purification via Immobilized Metal Affinity Chromatography (IMAC). **(A)** Chromatographic purification profile and **(B)** SDS-PAGE analysis of the IMAC purification fractions.
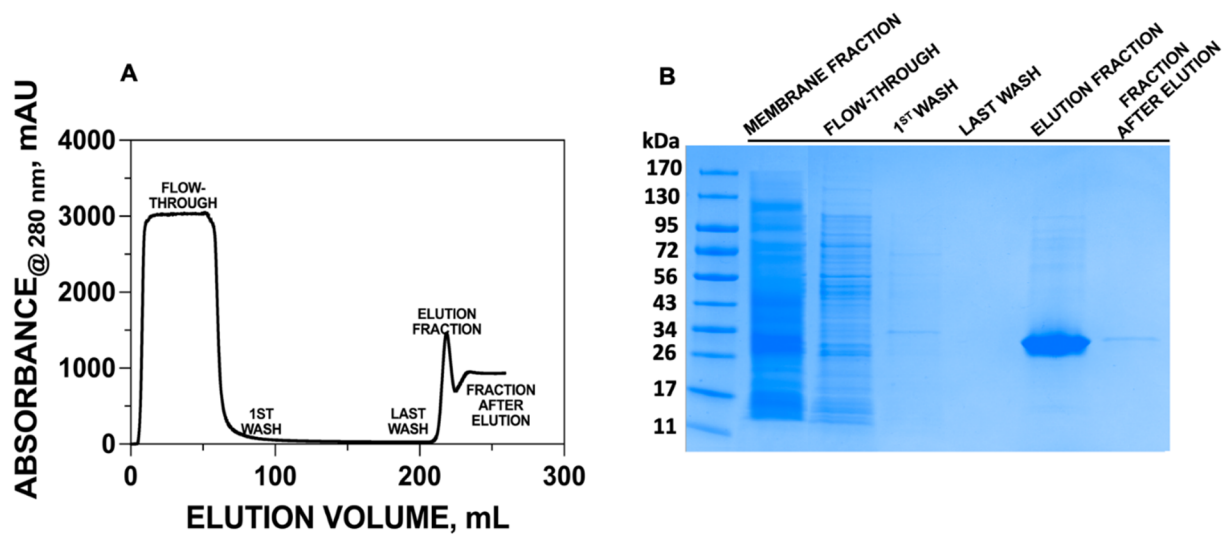
Figure S3. Emission spectra (λ_{exc} = 480 nm, slit width= 2.5 nm; λ_{em} = 515 nm; slit width= 2.5 nm) of FluoZin-3-Zn(II) complex (10 µM) titrated with Ni(II) (left) and Co(II) (right) in the presence of liposomes (total lipid concentration 25 mg/ml). The expected metal swap reaction generating FluoZin-3-Ni(II) or FluoZin-3-Co(II), together with potential collisional quenching contributions, results overall in fluorescence signal quenching.
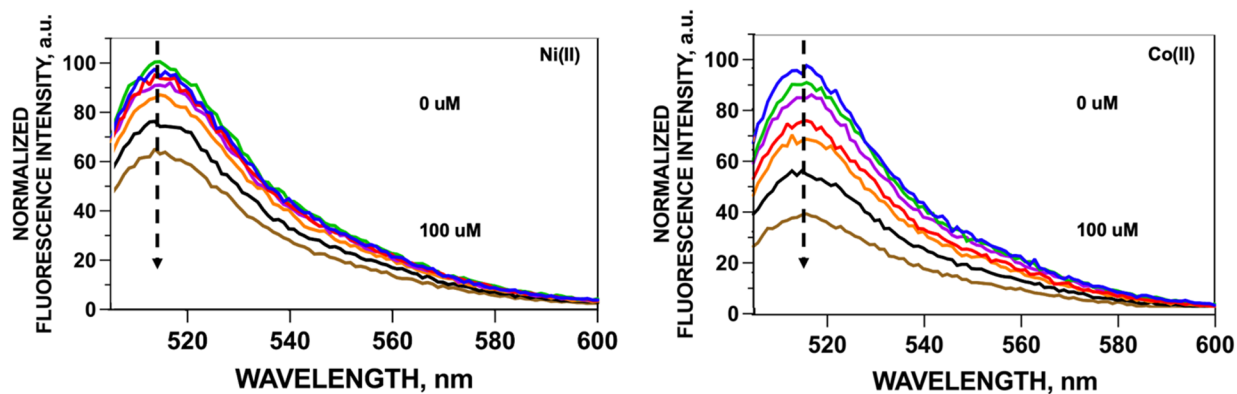
Figure S4. SDS-PAGE of purified NixA mutants after SEC and corresponding Western Blot analysis (* = samples after IMAC) utilizing an anti-His$_6$ tag monoclonal antibody, confirming similar purity, stability, and absence of degradation, as observed for wtNixA. Lane pictures for different mutants have been obtained from independent gels for each construct and assembled in a single figure for comparative analysis (for Western Blot, samples blotted on the same membrane are clustered with brackets).
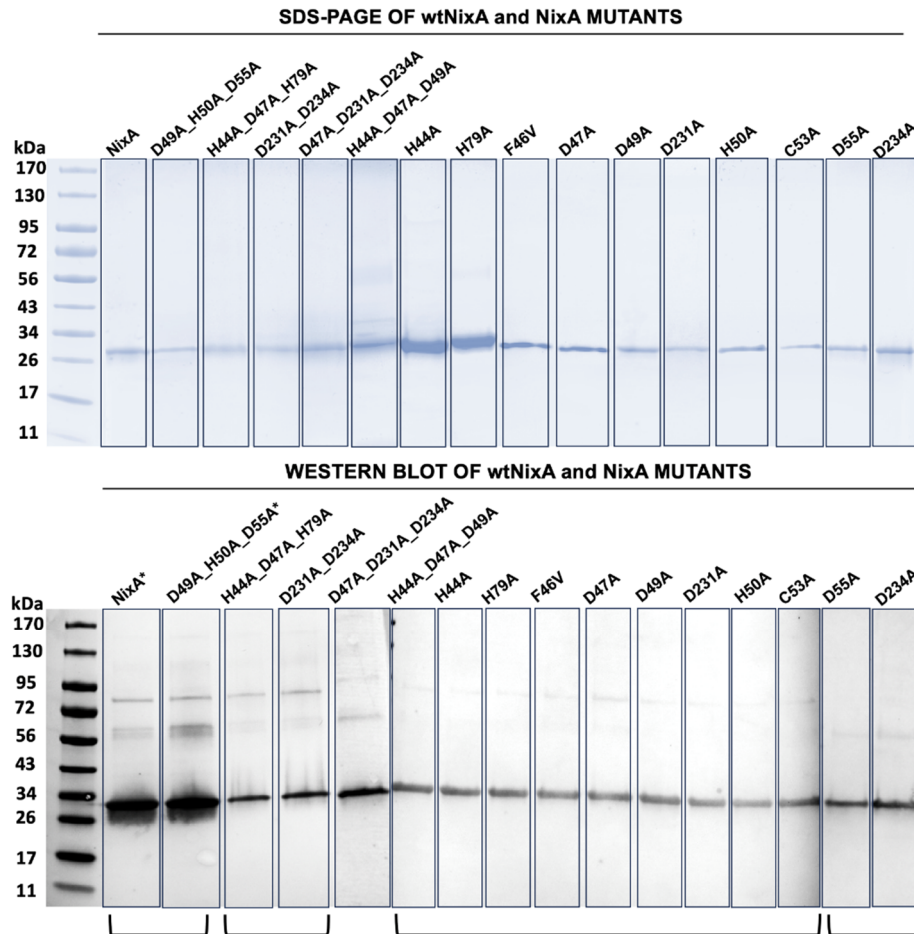
Figure S5. NixA mutation studies. (**A**) Maximum equilibrium fluorescence quenching signal upon Ni(II) transport in NixA and combination mutants proteoliposomes, monitored with FZ-3-Zn(II) encapsulated in the SUV lumen (25 μM; λ_{exc} = 480 nm, slit width= 2.5 nm; λ_{em} = 515 nm, slit width= 2.5 nm;) (n = 3). (**B**) Maximum equilibrium fluorescence quenching signal for Ni(II) transport in NixA proteoliposomes and single-point mutants monitored with FZ-3-Zn(II) encapsulated in the SUV lumen (25 μM; λ_{exc} = 480 nm; λ_{em} = 515 nm;) (n = 3).
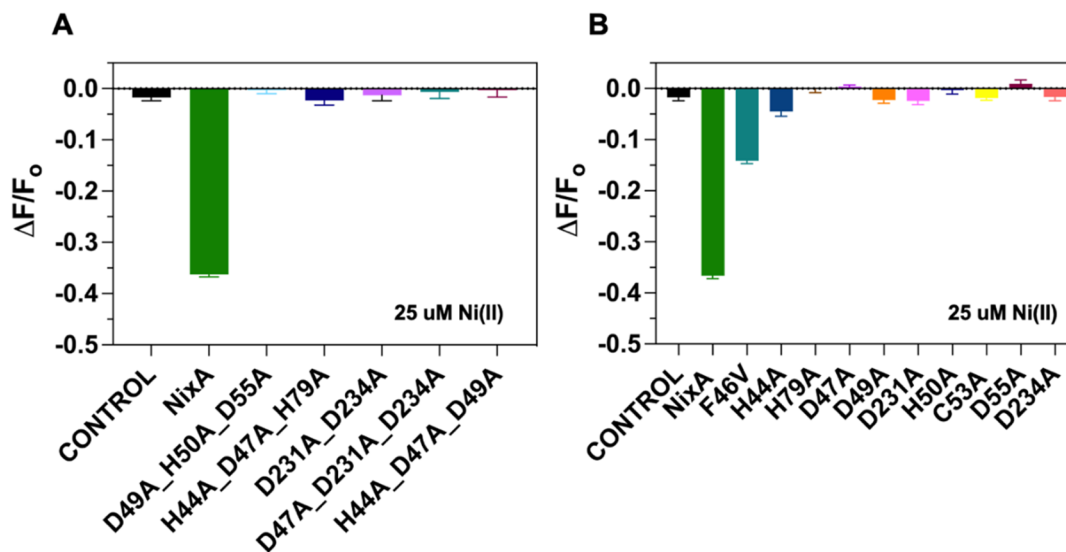
Figure S6: Distribution of chemical species according to the stoichiometric equilibrium (SE) binding model. M and A are the molar concentrations of NixA and Ni(II), respectively.
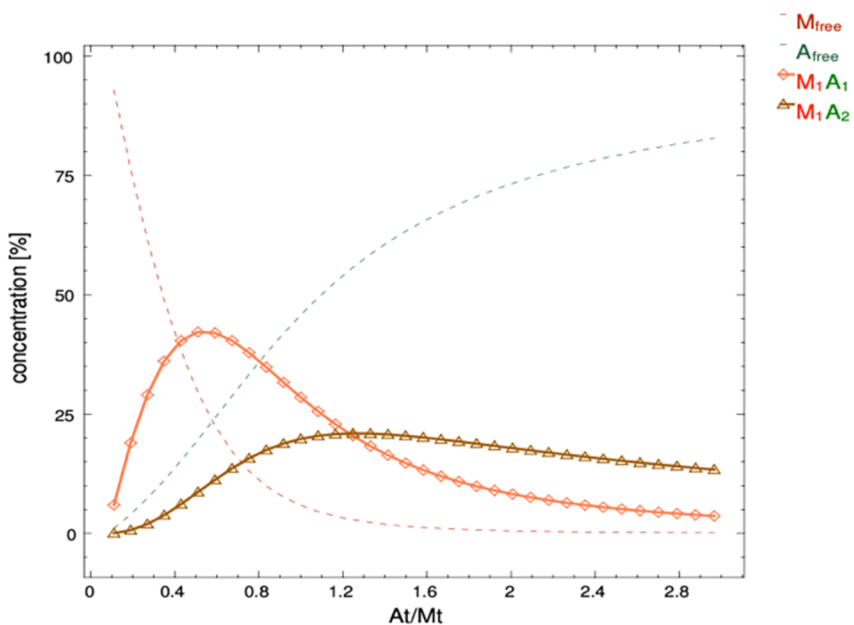

Figure S7: Contribution of complexes formation to the overall binding isotherm according to the stoichiometric equilibrium (SE) binding model. M and A are the molar concentrations of NixA and Ni(II), respectively.
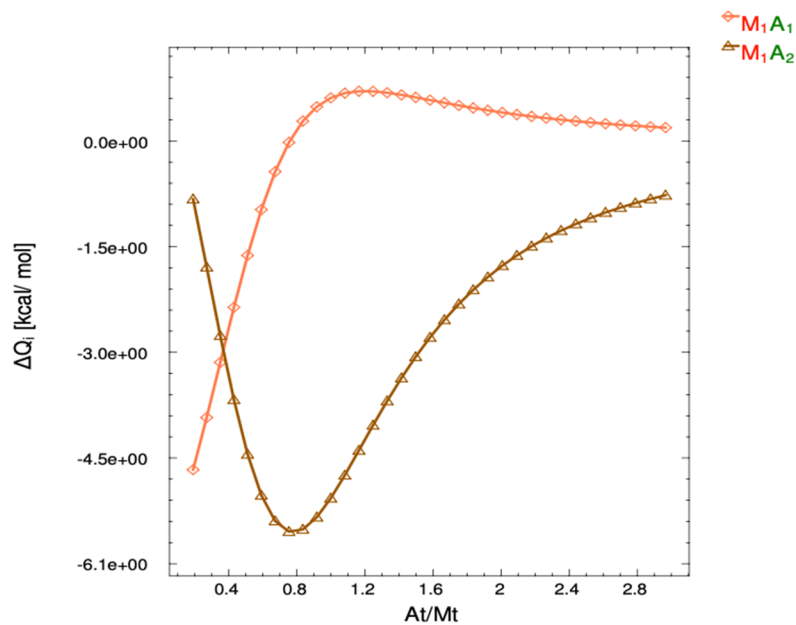
Figure S8: Distribution of chemical species, shown as fraction of sites occupied, according to the independent sites (IS) binding model. A[#1] and A[#2] are the molar fractions of the two Ni(II)-binding sites on NixA.
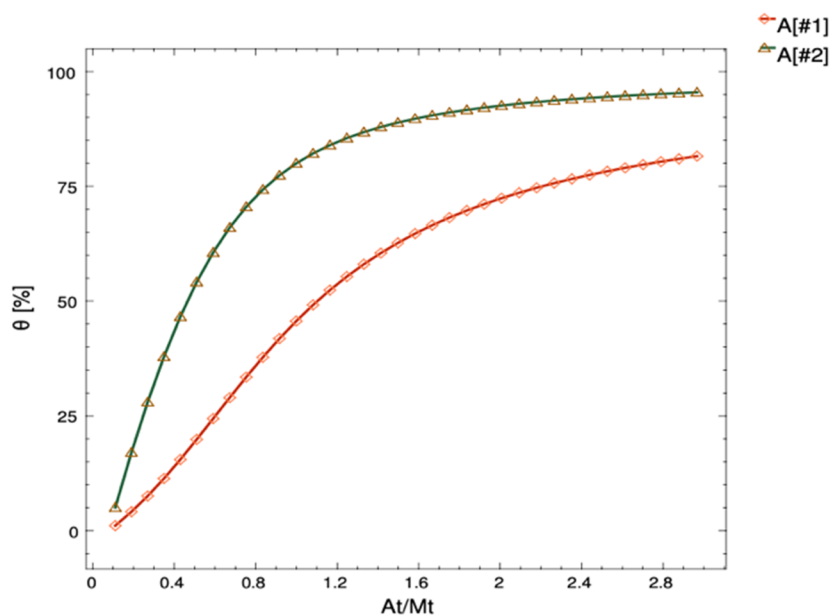

Figure S9: Contribution of complexes formation to the overall binding isotherm according to the independent sites (IS) binding model. A[#1] and A[#2] are the molar fractions of the two Ni(II)-binding sites on NixA.
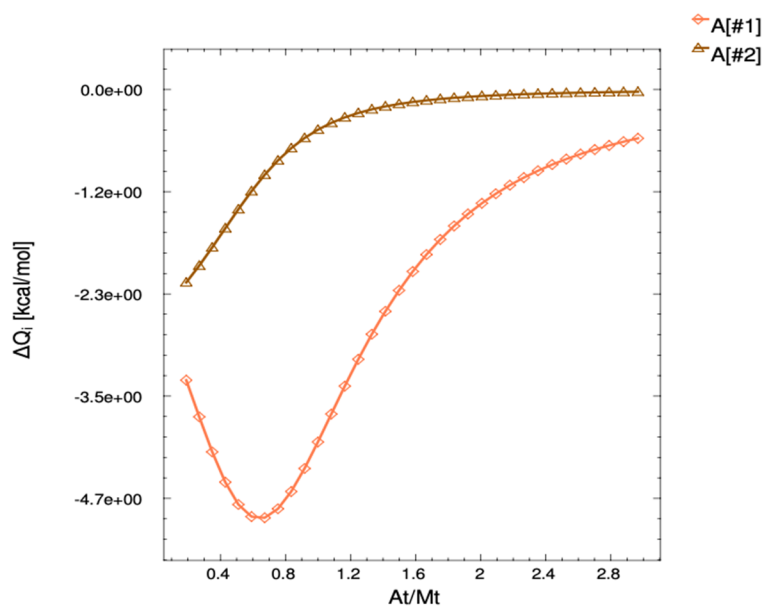
Table S1 Sequencing primers for NixA mutant constructs

NixA MUTANTS	Primer 1 (5'→3')	Primer 2 (5'→3')
H44A/D47A/D49A; H44A/D47A/H79A; D47A/D231A/D234A; D49A/H50A/D55A; D231A/D234A	CTGAAAATCTTCAAGAAAAG	TAATACGACTCACTATAGGG
H44A	TAATACGACTCACTATAGGG	AAAATCTTCAAGAAAAGCCA
D47A; D49A; C53A; D55A; D234A	AAAATCTTCAAGAAAAGCCA	TAATACGACTCACTATAGGG
F46V; H50A; H79A; D231A	AAATCTTCAAGAAAAGCCAC	TAATACGACTCACTATAGGG

Table S2. NixA and NixA mutants apparent initial Ni(II) transport velocities (absolute initial slopes). Values $< 1 \times 10^{-4}\,\text{s}^{-1}$ indicate that no significant transport is detected (n.d.)

NixA MUTANTS	$*\delta F/\delta t,\ \text{s}^{-1}$ $(25\ \mu\text{M Ni}^{2+})$
CONTROL (for NixA combination mutants)	n.d. $(3.9 \pm 2.8 \cdot 10^{-5})$
wild-type **NixA**	$\mathbf{2.80 \pm 0.70 \cdot 10^{-3}}$
D49A/H50A/D55A	n.d. $(4.3 \pm 0.3 \cdot 10^{-5})$
H44A/D47A/H79A	n.d. $(7.0 \pm 2.3 \cdot 10^{-5})$
D231A/D234A	n.d. $(6.0 \pm 2.6 \cdot 10^{-5})$
D47A/D231A/D234A	n.d. $(9.0 \pm 1.6 \cdot 10^{-5})$
H44A/D47A/D49A	n.d. $(8.0 \pm 2.4 \cdot 10^{-5})$
CONTROL (for NixA point mutants)	n.d. $(3.9 \pm 3.0 \cdot 10^{-5})$
H44A	n.d. $(4.7 \pm 2.0 \cdot 10^{-5})$
H79A	n.d. $(2.0 \pm 3.0 \cdot 10^{-5})$
F46V	$\mathbf{1.0 \pm 0.6 \cdot 10^{-3}}$
D47A	n.d. $(1.6 \pm 4.0 \cdot 10^{-5})$
D49A	n.d. $(6.0 \pm 0.5 \cdot 10^{-5})$
D231A	n.d. $(3.5 \pm 1.0 \cdot 10^{-5})$
H50A	n.d. $(1.5 \pm 3.0 \cdot 10^{-5})$
C53A	n.d. $(6.3 \pm 3.0 \cdot 10^{-5})$
D55A	n.d. $(6.4 \pm 5.0 \cdot 10^{-6})$
D234A	n.d. $(7.4 \pm 2.0 \cdot 10^{-6})$

Table S3. List of parameters obtained from a fit of the binding isotherm using the stoichiometric equilibrium (SE) or the independent sites (IS) models.

	Stoichiometric equilibrium (SE) model	Independent sites (IS) model
GoF (%)[a]	78.4	78.4
Qdil (cal mol^{-1})[b]	8.91e+1	8.91e+1
r_M[c]	0.44	0.44
n_1	1	1
n_2	1	1
K_{a1} (M^{-n})	7.6e+5	6.3e+5
K_{d1} (μM)	1.3	1.6
K_{a2} (M^{-n})	1.1e+5	1.3e+5
K_{d2} (μM)	9.1	7.7
ΔH_1 (cal mol^{-1})	-6.2e+3	-3.3e+3
ΔH_2 (cal mol^{-1})	-1.7e+4	-2.0e+4
ΔG_1 (cal mol^{-1})	-8.0e+3	-7.9e+3
ΔG_2 (cal mol^{-1})	-6.9e+3	-7.0e+3
ΔS_1 (cal mol^{-1} K^{-1})	6.0	15.5
ΔS_2 (cal mol^{-1} K^{-1})	-34.0	-43.7

[a]: Goodness of fit
[b]: Parameter that corrects for the molar enthalpy of dilution of the injected solute, generally required when no complementary dilution experiment (with the pure solvent in the cell) were performed and subtracted from a binding experiment
[c]: Scaling parameter employed to correct for potential differences between nominal and true concentration of protein in the sample cell